BMC Medicine

RESEARCH

Open Access

Gut microbiota-derived glutathione from metformin treatment alleviates intestinal ferroptosis induced by ischemia/reperfusion

Fangyan Wang[1†], Xinyu Wang[2†], Chaoyi Wang[3†], Wangxin Yan[4†], Junpeng Xu[1], Zhengyang Song[5], Mingli Su[3], Jingjing Zeng[1], Qiannian Han[1], Gaoyi Ruan[3], Eryao Zhang[3] and Wantie Wang[1*]

Abstract

Background Intestinal ischemia/reperfusion injury (IIRI) is a life-threatening condition caused by multiple organ and system failures induced by dysbiosis and gut leakage. Metformin has demonstrated efficacy in protecting against IIRI, although the precise role of the gut microbiota in the underlying mechanism is still ambiguous.

Methods This study examined intestinal barrier function and ferroptosis-related parameters in mice with IIRI following treatment with metformin. Additionally, dirty cages and antibiotics were utilized to investigate the impact of the microbiota on the effects of metformin. The analysis included an assessment of the microbial composition of metformin-treated mice and the biosynthetic activity of specific metabolites.

Results Metformin effectively reduced gut leakage induced by IIRI, as evidenced by decreased intestinal permeability and increased Occludin, ZO-1, Claudin-1, and MUC-1 expression. A decrease in the expression of the pro-ferroptotic proteins ACSL4, TFR1, and VDAC2/3 and a decrease in dihydroethidium (DHE) fluorescence, iron, malondialdehyde (MDA), and myeloperoxidase (MPO) were further observed in metformin-treated mice. In contrast, the damage to the GPX4/GSH system caused by IIRI was reversed after metformin treatment, as shown by increases in GPX4, SLC7A11, and GSH. The antiferroptotic effects of metformin were phenocopied by its fecal microbiota but were eliminated by antibiotic intake. 16S rRNA analysis revealed that the metformin-modulated gut microbiota was characterized by increased *Lactobacillus murinus*, which expressed higher levels of GshF that contributed to the mitigation of IIRI.

Conclusions Murine gut microbiota mediated the anti-ferroptotic effect of metformin on IIRI, and the resulting increase in microbial GSH synthesis could serve as a critical pathway for anti-IIRI.

Keywords Metformin, Intestinal ischemia/reperfusion injury, Ferroptosis, Gut microbiota, Glutathione

†Fangyan Wang, Xinyu Wang, Chaoyi Wang and Wangxin Yan contributed equally to this work and share first authorship.

*Correspondence:
Wantie Wang
wwt@wmu.edu.cn
Full list of author information is available at the end of the article

Background

Intestinal ischemia/reperfusion injury (IIRI) is a life-threatening condition that results from sudden deprivation of intestinal blood flow and systemic diseases, such as incarcerated hernia [1], intestinal transplantation [2], hemorrhagic shock [3], and sepsis [4]. If not properly controlled, IIRI can trigger substantial dysfunction of the intestinal barrier, known as gut leakage, that can lead to multiple organ disorders [5]. However, the lack of targeted therapies in clinical practice contributes to a poor prognosis for patients with IIRI, which has a high mortality rate of 50–69% [6].

Recent studies have shown that ferroptosis, a type of cell death characterized by lipid peroxidation, is a crucial factor in the pathogenesis of IIRI. Ischemia/reperfusion (IR) increases the expression of acyl-CoA synthetase long-chain family member 4 (ACSL4) in intestinal tissue, which initiates ferroptosis. This process is also typically accompanied by the inhibition of glutathione peroxidase 4 (GPX4) and glutathione (GSH) systems, which normally eliminate lipid peroxides [7, 8]. Notably, several studies have shown that IIRI can be significantly mitigated by blocking ferroptosis with exogenous antioxidants such as resveratrol or by promoting GPX4 expression through the activation of transient receptor potential vanilloid 1 (TRPV1) in animal models [9, 10]. However, further research is needed to explore possible strategies for inhibiting ferroptosis in IIRI clinical therapy.

Gut microbiota play a crucial role in maintaining the intestinal barrier [11]. Ischemia and hypoxia can disrupt the microbial composition of the gut microbiome, which can lead to intestinal barrier dysfunction and bacterial translocation [12]. Efforts to alleviate IIRI by modulating the microbiota, such as with probiotic *Bifidobacterium* and *Lactobacillus plantarum* transplantation in animal models, have already been reported [13, 14]. Additionally, microbiota-derived capsiate has been found to inhibit Intestinal ischemia/reperfusion (IIR)-induced ferroptosis effectively by up-regulating GPX4 [10]. This initial evidence suggests that regulating the gut microbiota may be an effective strategy to combat intestinal ferroptosis induced by IR.

Metformin (Met), a first-line medication for type 2 diabetes, has been shown to protect against IIRI in mice by reducing oxidative stress [15]. When taken orally, metformin is concentrated in the intestine at levels up to 300 times greater than in the blood, significantly influencing the composition and metabolism of the gut microbiota [16]. Research has also demonstrated that metformin increases the abundance of *Akkermansia muciniphila* in the gut, which triggers the transcription of host antioxidant genes, including *Nqo1*, *Ho-1*, and *Gpx4* [17]. Li et al. have reported that metformin combined with probiotic-derived outer membrane vesicles can modulate the gut microbiota and eliminate excess reactive oxygen species (ROS) in a murine inflammatory bowel disease (IBD) model [18]. However, the specific antioxidative metabolites produced by metformin-treated microbiota and their anti-IIRI effects have not been fully elucidated.

In this study, we administered metformin to mice in order to assess changes in the intestinal barrier, cell ferroptosis, microbial composition, and metabolites in a mouse model of IIRI. Our findings lend support to a novel pharmacological approach and demonstrate that metformin can serve as a promising therapeutic agent for IIRI by enhancing the production of microbial GSH, thereby mitigating intestinal ferroptosis.

Methods

Animals

Male C57BL/6 mice (6–8 weeks old, 18–22 g) were purchased from Beijing Weitonglihua Experimental Animal Technology Co., Ltd. (Beijing, China). The mice were traceable for quality and health status, and had not undergone any procedures before. The mice were housed in conditions were controlled with a temperature range of 20–24 °C, humidity maintained at 50–60%, and a 12-h light–dark cycle, with free access to food and water. Exclusion criteria were predefined: signs of illness, significant weight loss (> 10%), or other accidents during the study were excluded. No mice in our study met the exclusion criteria. All animal experiments got approval from the Experimental Animal Center of Wenzhou Medical University.

Mice were randomly assigned to the six experimental groups using a computer-generated random sequence: (1) Control group: sham surgery without additional treatment; (2) IIRI group: subjected to IIRI surgery; (3)

(See figure on next page.)

Fig. 1 Metformin-induced impairment of intestinal barrier function. **A** H&E staining of mouse ileum tissues. Magnification, 200 × and 400 ×. Scale bar = 50 μm. **B** FITC-dextran concentration in the blood of the mice. **C**-**E** qRT-PCR analysis of IL-1β, IL-18, and IL-6 I liver. **F** ZO-1, Occludin, Claudin-1, and MUC mRNA expression in ileum tissues. **G** Western blot analysis of ZO-1 and Occludin expression. **H**-**I** Quantitative analysis of the Western blot results. **J** Immunofluorescence image of ZO-1 in ileum tissues. Magnification 400 ×. Scale bar = 50 μm. **K** Quantitative analysis of fluorescence intensities. The data are presented as the means ± SEMs ($n = 6$/group for **B**-**F** and $n = 3$/group for **G**-**K**). * $p < 0.05$, ** $p < 0.01$, *** $p < 0.001$, **** $p < 0.0001$

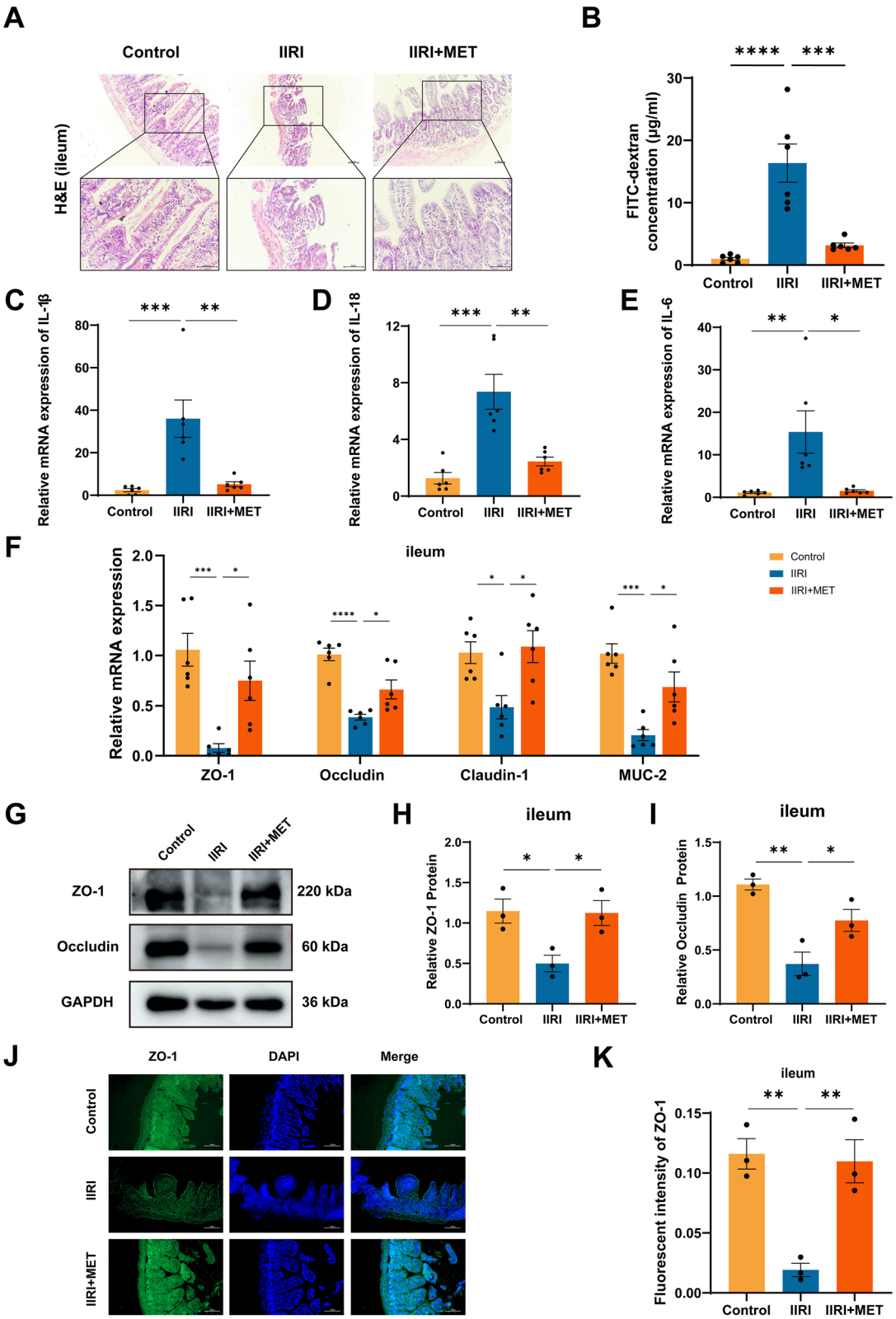

Fig. 1 (See legend on previous page.)

IIRI + MET group: treated with metformin (1 mg/mL in drinking water) for one week prior to IIRI; (4) Dirty cage group: housed below a partially hollowed MET group cage, ingesting feces from MET-treated mice for one week; (5) IIRI + MET + Abx group: administered oral antibiotics (ampicillin 1 g/L, neomycin 1 g/L, metronidazole 1 g/L, and gentamicin 160 mg/L) combined with metformin in drinking water for one week prior to IIRI; (6) IIRI + LM group: received 0.1 mL/10 g of Lactobacillus murinus (1×10^9 CFU/mL) daily via gavage for one week prior to IIRI surgery. A total of 52 mice were used in the study. Groups 1–5 consist of 6 mice, and 6 extra mice were included in groups 1–3 exclusively for the FITC permeability test. Group 6 consists of 4 mice, as prior experiments showed acceptable variability. Investigators performing assessment were blinded to group allocations. The order of treatments and measurements was also randomized. A schematic diagram detailing group assignments and experimental procedures is provided in Additional File 1: Figure S1.

IIRI surgery

Mice were weighed and anesthetized with 50 mg/kg pentobarbital sodium salt (Merck, Tc-P8411) after a 12-h fast. A 2–3 cm midline abdominal incision was made to expose the superior mesenteric artery (SMA), which was then clamped for 30 min. The clamp was then removed to restore SMA blood flow. The mice were sacrificed after 1 h of reperfusion for sampling. In the sham surgery, adipose tissues were clamped for 30 min instead of the SMA.

Dirty cage

Dirty cages were placed beneath the cages of IIRI + MET mice. The floor of the IIRI + MET cage is divided into two parts, with one half covered with bedding and the other half left uncovered and hollowed. Mice prefer to live on bedding but tend to excrete on the uncovered grid area, allowing fresh feces to fall into the dirty cage and ingested by the mice.

H&E staining

Ileum tissues were removed immediately after sacrifice, fixed in 10% formalin for 24 h, and embedded in paraffin. The tissue samples were sliced into approximately 5-μm-thick sections and stained with hematoxylin and eosin (H&E) (Solarbio, Beijing, China). An optical microscope (Olympus, Tokyo, Japan) was used to observe pathological changes.

Intestinal permeability test

Mice were orally administered 0.5 mL of 25 mg/mL 4 kDa fluorescein isothiocyanate (FITC)-dextran (Merck, 46,944) in sterile water 30 min prior to sacrifice. Changes in intestinal permeability were assessed by measuring serum samples collected via the retro-orbital sinus. Absorbance was recorded at 490 nm using a fluorospectrometer.

Assessment of MDA, GSH and MPO

Fresh tissue homogenate was mixed with 5,5'-dithio-bis2-(nitrobenzoic acid) and reacted with GSH to produce yellow-colored 5-thio2-nitrobenzoic acid (TNB). GSH was quantified by measuring the absorbance at 412 nm. Tissue homogenate supernatant mixed with thiobarbituric acid was used to evaluate the malondialdehyde (MDA) content by measuring the absorbance at 532 nm. Myeloperoxidase (MPO) activity was determined by measuring the absorbance at 460 nm after incubating the homogenate supernatant in the reaction solution and adding 50 μL of hydrogen peroxide. The assays were conducted using kits from the Nanjing Jiancheng Bioengineering Institute (Nanjing, China), and the absorbance was measured with a spectrophotometer.

Iron assay

The iron concentration was determined using an iron assay kit (Nanjing Jiancheng Bioengineering Institute, Nanjing, China). The tissue homogenate supernatant was mixed with chroFmogenic reagents and boiled for 5 min. The iron concentration was calculated based on the absorbance at 520 nm using a spectrophotometer.

Quantitative real-time PCR (qRT-PCR) of mRNA and microbial DNA

Total RNA from tissues was extracted using TRIzol reagent (Yamei, Shanghai, China) and reverse-transcribed into complementary DNA (cDNA) with a reverse

(See figure on next page.)

Fig. 2 The alleviation of ferroptosis in IIRI by metformin. **A** Immunofluorescence of DSH in mouse ileum tissues. Magnification 400 ×. Scale bar = 50 μm. **B**, **C** MDA and GSH concentrations in all groups. **D** MPO activity in all groups. **E** Iron concentration in all groups. **F** The mRNA expression of SLC7 A11 and GPX4 in ileum tissues. **G** The mRNA expression of ACSL4, TFR1, and VDACs in ileum tissues. **H** Western blot analysis of ACSL4, TFR1, SLC7 A11, GPX4 and VDACs. **I** Quantitative analysis of the Western blot results. **J** Western blot analysis of AMPK. The data are presented as the means ± SEMs ($n = 6$/group for **B**-**G** and $n = 3$/group for **A**, **H**-**J**). * $p < 0.05$, ** $p < 0.01$, *** $p < 0.001$, **** $p < 0.0001$

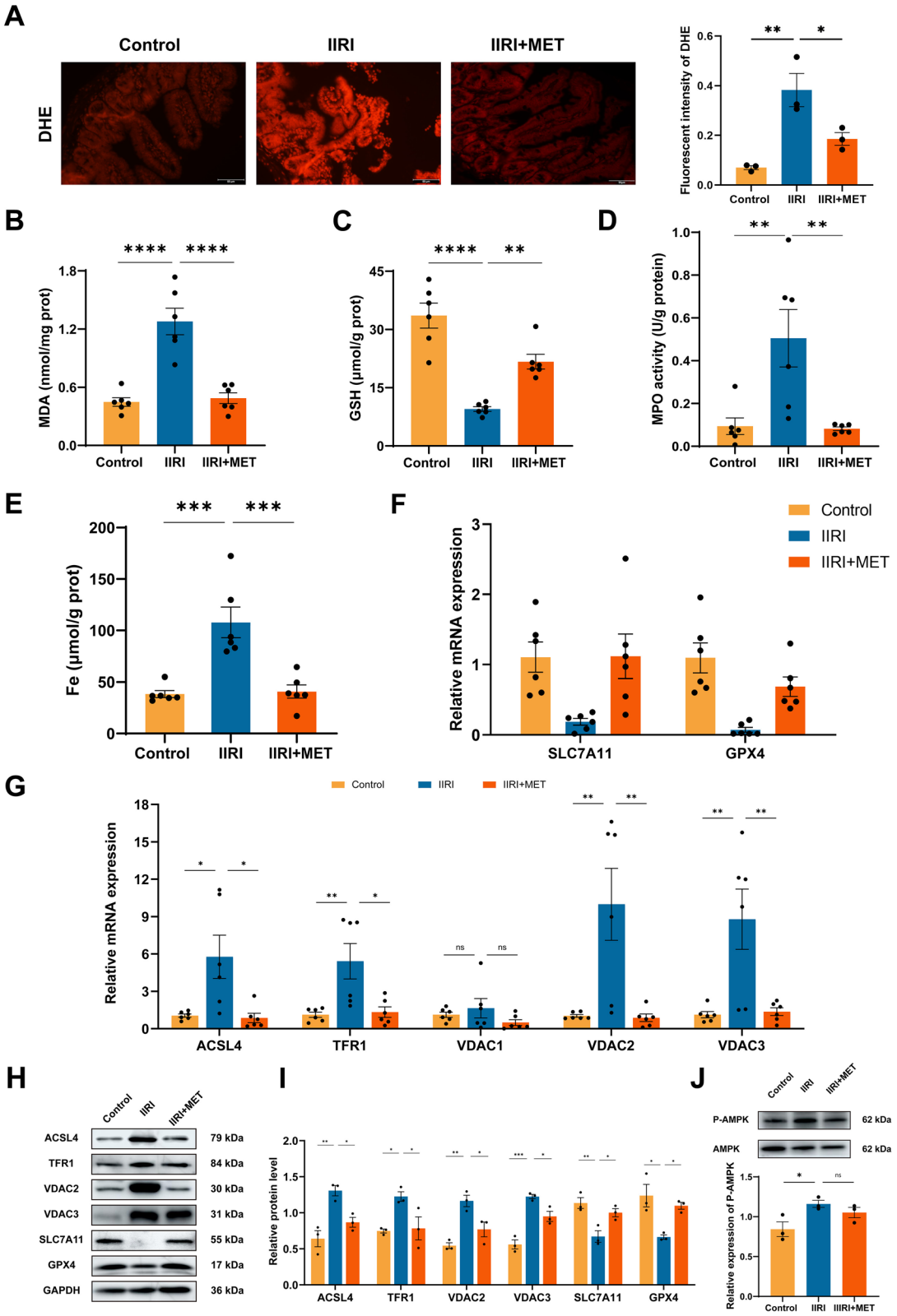

Fig. 2 (See legend on previous page.)

transcription kit (Vazyme, Nanjing, China). Microbial DNA was extracted using a Bacterial Genome DNA Extraction Kit (Generay Biotechnology, Shanghai, China). PCR was performed using primers for ZO-1, Occludin, Claudin-1, Mucin 2 (MUC-2), ACSL4, transferrin receptor 1 (TFR1), solute carrier family 7 member 11 (SLC7 A11), GPX4, and voltage-dependent anion channels (VDACs) 1, 2, 3. The relative mRNA expression was evaluated using the Thermal Cycler Dice Real-Time System (TaKaRa Company, Japan) and the SYBR Green Kit (Vazyme, Nanjing, China). The sequences of primers used are listed in Additional file 2: Table S1.

Western blot

Proteins were extracted using RIPA lysis buffer and a tissue grinder. Protein concentration was subsequently determined using the BCA assay. 20 μg of protein were loaded onto SDS-PAGE gels, and proteins were separated based on their molecular weight through electrophoresis. The proteins were then transferred onto PVDF membranes using a semi-dry transfer system. The membranes were blocked with 5% BSA and incubated with primary antibodies at 4 °C for 12 h, followed by secondary antibodies (HRP-conjugated Goat Anti-Mouse IgG, Proteintech, SA00001-1, 1:20000) for 1 h at room temperature. Protein bands were visualized using an Odyssey imaging system (LI-COR Biosciences, NE). The primary antibodies used included anti-ZO-1 (Abcam, ab307799, 1:5000), anti-Occludin (Abcam, ab216327, 1:5000), anti-ACSL4 (Abcam, ab155282, 1:10000), anti-TFR1 (ABclonal, A5865, 1:2000), anti-SLC7 A11 (Abcam, ab175186, 1:5000), anti-GPX4 (Abcam, ab125066, 1:5000), anti-VDAC2 (Proteintech, 11663–1-AP, 1:5000), anti-VDAC3 (Proteintech, 55260–1-AP, 1:5000), β-tubulin (Proteintech, 10068–1-AP, 1:5000), and GAPDH (Proteintech, 10494–1-AP, 1:20000).

16S rDNA gene sequencing analysis

Fresh ileum contents were collected for analysis, and specific primers with barcodes are used to amplify the V3 to V4 variable regions of the bacterial 16S rDNA via PCR. The PCR products were quantified, adapter sequences were added, and the products were purified. After purification, the DNA was then denatured for library construction and sequenced via next-generation sequencing (NGS). OTU clustering, diversity metrics, taxonomic classification, and multivariate community composition analysis were conducted to examine the microbial community structure and phylogeny.

Immunofluorescence staining

The paraffin-embedded sections were deparaffinized and subjected to antigen retrieval in a boiling sodium citrate solution (0.01 mol/L, pH 6.0). Following this, the samples were sequentially incubated with primary and secondary antibodies, and nuclei were stained with 4',6-diamino-2-phenylindole (DAPI) (Beyotime Biotechnology, China). Imaging was then conducted using laser scanning confocal microscopy, which provided high-resolution images for detailed analysis, and the results were subsequently quantified using ImageJ software (National Institute of Mental Health, Bethesda, MD, USA).

Bacterial strains and culture

Lactobacillus murinus freeze-dried powder (BeNa Culture Collection, Beijing, China) was dissolved in 25 ml of MRS broth (Hope Bio-Technology, Qingdao, China). The mixture was incubated at 37 °C under anaerobic conditions for 24 h and then diluted with MRS broth to a concentration of 10^8 CFU/L using a spectrophotometer. The broth was subcultured with L-N-acetylcysteine (L-NAC) at a concentration of 2 mg/ml. A control group without L-NAC was used for comparison. The GSH concentration was measured over 90 min under 37 °C anaerobic culture.

Statistical analysis

All data from this study were collected and analyzed using GraphPad Prism 9 software and are presented as the mean ± standard error of the mean (SEM). The normality of the data was assessed using the Shapiro–Wilk test. For data that followed a normal distribution, one-way analysis of variance (ANOVA) was used to evaluate discrepancies among multiple groups. For data that did not follow a normal distribution, the Kruskal–Wallis test was applied. Statistical significance was defined as $p < 0.05$ for all comparisons.

Results

Metformin reduced the damage to intestinal barrier function induced by IIRI

Given the critical risks of IIRI-induced gut leakage to multiple bodily systems, we investigated changes in the intestinal barrier in metformin-treated mice. Metformin

(See figure on next page.)

Fig. 3 Dirty cage treatment suppressed ferroptosis in IIRI mice. **A** H&E staining of mouse ileum tissues. Magnification, 200 × and 400 ×. Scale bar = 50 μm. **B** FITC-dextran concentration in the blood of mice. **C** The mRNA expression of ZO-1 and Occludin in ileum tissues. **D**-**F** Western blot image and quantitative analysis of ZO-1 and Occludin. **G** Immunofluorescence image and quantitative detection of DHE in ileum tissues. Magnification 400 ×. Scale bar = 50 μm. **H** Comparison of the ileum iron concentration between the groups. **I**, **J** qRT-PCR analysis of ACSL4, TFR1, SLC7 A11, GPX4 and VDACs. **K**, **L** Western blot image and quantitative analysis of ACSL4, TFR1, SLC7 A11, GPX4, and VDACs. The data are presented as the means ± SEMs ($n = 6$/group for **B**-**C**, **H**-**J** and $n = 3$/group for **D**-**G**, **K**-**L**). * $p < 0.05$, ** $p < 0.01$, *** $p < 0.001$, **** $p < 0.0001$

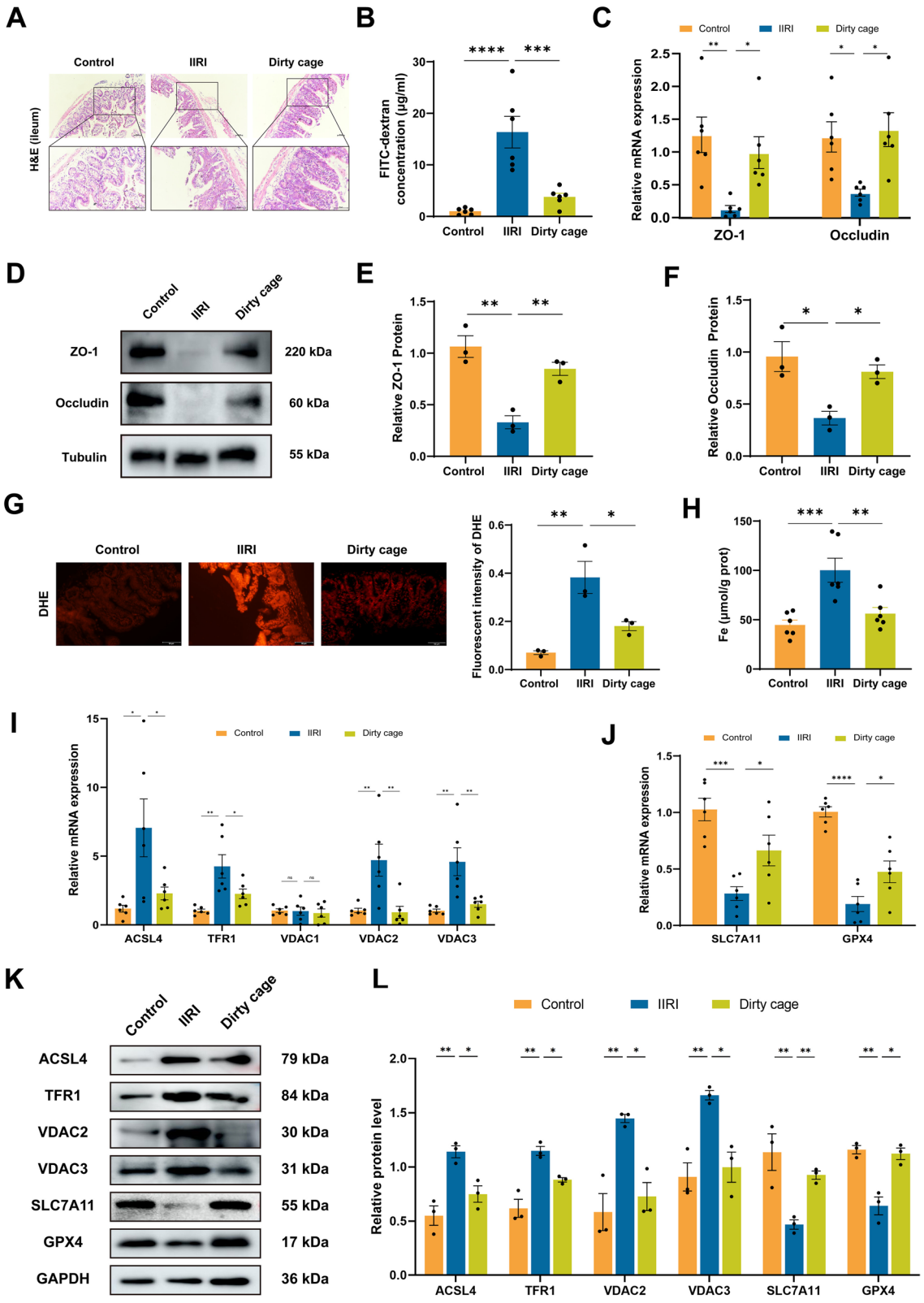

Fig. 3 (See legend on previous page.)

treatment significantly reversed the shedding of the villus tips and the exposure of the basal membrane caused by IIRI, as revealed by H&E staining (Fig. 1A). Treatment with metformin prevented the oral administration of FITC-dextran, which is concentrated in the bloodstream in the IIRI group, from crossing the intestinal barrier ($p < 0.001$, Fig. 1B), indicating the restoration of intestinal function. Correspondingly, liver mRNA levels of interleukin (IL)−1β, IL-18, and IL-6 were upregulated, showing an activated inflammatory response led by leaky gut. Furthermore, qRT-PCR of tight junction proteins and mucins, which are essential for maintaining the intestinal barrier, revealed that the reductions in the expression of ZO-1, Occludin, Claudin-1, and MUC-2 in the IIRI model were markedly increased by metformin treatment ($p < 0.05$, Fig. 1F). The western blotting results for ZO-1 and Occludin were consistent with their mRNA expression ($p < 0.05$, Fig. 1G-I). Immunofluorescence showed that metformin treatment significantly restored ZO-1 expression ($p < 0.01$, Fig. 1J and K). Overall, metformin treatment significantly attenuated barrier dysfunction induced by the IIR through increased expression of ZO-1, Occludin, Claudin-1, and MUC-2.

Metformin alleviated intestinal ferroptosis in IIRI

Considering the role of ferroptosis in the development of IIRI, we designed a series of experiments to observe intestinal ferroptosis in that specific context. Dihydroethdium (DHE) fluorescence intensity in tissues was increased in the IIRI model group but was notably reduced by metformin ($p < 0.0001$, Fig. 2A). Metformin significantly decreased the elevated MDA levels and MPO activity observed in IIRI mice ($p < 0.0001$ or $p < 0.01$, Fig. 2B and D), indicating a reduction in peroxide levels. The evaluation of iron metabolism showed that metformin attenuated iron accumulation in the ileum of IIRI mice ($p < 0.001$, Fig. 2E). qRT-PCR and Western blotting further confirmed the antiferroptosis effect through the significant downregulation of ACSL4 and TFR1 ($p < 0.05$, Fig. 2G-I) and upregulation of SLC7 A11 ($p < 0.05$, Fig. 2F and H) in the metformin-treated group. Additionally, measurement on the GSH/GPX4 system revealed increases in GSH content and GPX4 expression in metformin-treated mice compared to those in IIRI model mice ($p < 0.05$, Fig. 2C, F and H). VDAC1 mRNA and protein expression did not significantly differ between the groups, while VDAC2 and VDAC3 were significantly downregulated in metformin-treated IIRI mice ($p < 0.01$, $p < 0.05$, Fig. 2G-I). The protein expression of AMP-activated protein kinase (AMPK) did not significantly change after metformin treatment ($p > 0.05$, Fig. 2J). These results demonstrate that inhibiting ferroptosis, rather than activating the AMPK pathway, is the primary mechanism of action of metformin against IIRI.

Fecal matter from metformin-treated mice attenuates intestinal ferroptosis induced by IIRI

To investigate the role of the gut microbiota in the antiferroptosis effect of metformin, we established a dirty cage group by allowing mice to feed on metformin-modulated feces from the MET group. H&E staining revealed that fecal matter significantly reversed villus shedding and basal membrane exposure in the IIRI group (Fig. 3A). Correspondingly, treatment with metformin-modulated fecal microbiota led to a notable reduction in FITC-dextran leakage into the bloodstream and increased the expression of ZO-1 and Occludin ($p < 0.001$, $p < 0.01$ or $p < 0.05$, Fig. 3B-F). In terms of ferroptosis-related indicators, the abnormal DHE concentration ($p < 0.0001$, Fig. 3G) and increased iron level ($p < 0.05$, Fig. 3H) in the IIRI group were reversed by fecal treatment. Moreover, mice in the dirty cage group exhibited downregulation of ACSL4 and TFR1 ($p < 0.05$, Fig. 3I, K, and L) and upregulation of SLC7 A11 and GPX4 ($p < 0.05$, Fig. 3J-L) compared to those in the IIRI model group. Although VDAC1 did not significantly differ between groups (Fig. 3I), both VDAC2 and VDAC3 were downregulated at the mRNA and protein levels in response to fecal treatment ($p < 0.01$ or $p < 0.05$, Fig. 3I, K, and L). These findings indicate that metformin-modulated fecal matter mitigates IIR-induced intestinal ferroptosis, thereby ameliorating intestinal barrier dysfunction.

Antibiotics eliminated the efficacy of metformin against intestinal ferroptosis in IIRI

Metformin-treated IIRI mice were administered antibiotics to disrupt their gut microbiota. As expected, qRT-PCR and western blotting revealed that antibiotics eliminated the upregulation of ZO-1 and Occludin induced by metformin treatment ($p < 0.05$, $p < 0.01$, Fig. 4A, C, and D). Immunofluorescence confirmed the downregulation of ZO-1 in the ileum mucosa of the antibiotic-treated mice

(See figure on next page.)

Fig. 4 The antibiotics removed the anti-IIRI effect of metformin. **A** The mRNA expression of ZO-1 and Occludin in the different groups. **B** Immunofluorescence image of ZO-1 in ileum tissues. Magnification 400 ×. Scale bar = 50 μm. **C**, **D** Western blotting results showing ZO-1 and Occludin expression. **E** Immunofluorescence image and quantification of DHE concentrations in ileum tissues. Magnification 400 ×. Scale bar = 50 μm. **F**, **G** qRT-PCR analysis of ACSL4, TFR1, and GPX4. (H-I) Western blot image and quantification of ACSL4, TFR1, and GPX4 expression. The data are presented as the means ± SEMs ($n = 6$/group for **A**, **F**-**G** and $n = 3$/group for **B**-**E**, **H**-**I**). * $p < 0.05$, ** $p < 0.01$, *** $p < 0.001$, **** $p < 0.0001$

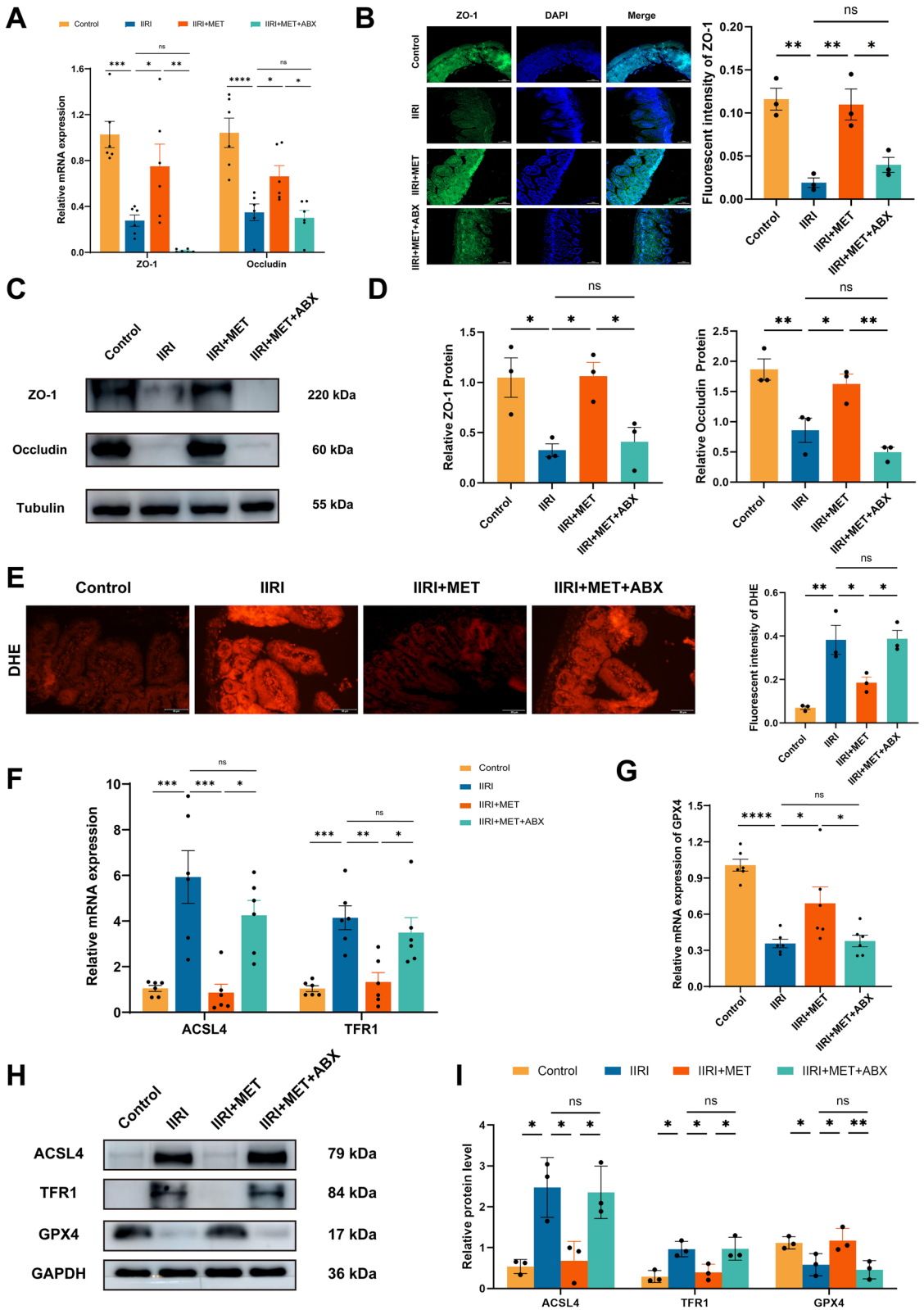

Fig. 4 (See legend on previous page.)

(Fig. 4B, $p < 0.05$). Further analysis revealed that antibiotics disrupted the antiferroptotic effect of metformin, with significant increase in DHE fluorescence led by antibiotic treatment ($p < 0.05$, Fig. 4E). Ferroptosis-related indicators from qRT-PCR and western blotting showed that IIRI + MET + Abx mice expressed increased ACSL4 and TFR1 and reduced GPX4 in compared to IIRI + MET mice at both the mRNA and protein levels—effects opposite to those induced by metformin ($p < 0.05$, $p < 0.01$, Fig. 4F-I). Overall, the effectiveness of metformin was compromised by the disruption caused by antibiotics, highlighting the essential role of metformin-modulated microbiota in counteracting intestinal ferroptosis.

Metformin increased ileal GSH synthesis

Given the close relationship between the gut microbiota and the antiferroptotic effect of metformin, 16S rDNA sequencing was performed on ilea content to investigate changes in the gut microbiota across the groups. The MET group had significantly greater alpha diversity metrics, including the Ace, Chao, and Shannon indices ($p < 0.05$, Fig. 5A-C), indicating an abundant and evenly distributed gut microbial community in the metformin-treated mice. Analysis of the microbial composition revealed that metformin treatment increased the abundance of Firmicutes and decreased the abundances of Actinobacteria and Proteobacteria at the phylum level (Fig. 5D). Specifically, *Lactobacillus murinus* was the most upregulated genus under metformin treatment (Fig. 5E). Further evaluation of metabolic models of the microbiota by examining 70 metabolic pathways from the KEGG database revealed a significant increase in the function of glutamate-cysteine ligase and GSH biosynthesis in the metformin-modulated microbiota (Fig. 5F). Consistent with the KEGG prediction, GSH levels in the ileum excrement of mice significantly increased (Fig. 5G, $p < 0.05$), and *Lactobacillus murinus* produced significantly more GSH in L-NAC broth than in blank broth (Fig. 5H, $p < 0.01$). GSH biosynthesis was identified by the mRNA levels of *GshF*, a critical amino acid ligase of the bifunctional pathway. The results showed that *GshF* was significantly upregulated after 30 min of culture, corresponding with the increase in GSH (Fig. 5I, $p < 0.01$). To confirm the anti-ferroptotic effects of *Lactobacillus murinus*, we investigated the IIRI + LM mice, which had been gavaged with it. The *Lactobacillus murinus* improved mucosal integrity, as indicated by histological expression in the ileum (Fig. 5K). Results showed decreased Fe levels and increased GSH levels in the ileum of the IIRI + LM mice (Fig. 5J, $p < 0.001$, $p < 0.0001$). Additionally, western blot analysis revealed reduced expression of ACSL4 and TFR1 (Fig. 5L-M, $p < 0.0001$), along with elevated GPX4 expression (Fig. 5L-M, $p < 0.001$), suggesting attenuated ferroptosis. These findings highlight that *Lactobacillus murinus* enhances microbial GSH synthesis pathways, thereby counteracting intestinal ferroptosis.

Discussion

Metformin has garnered significant attention for its potential therapeutic effects on various diseases, including IIRI, although the precise underlying mechanisms remain to be elucidated [15]. Our study demonstrated that the anti-ferroptosis effects of metformin are mediated by a modulated microbiota, specifically through the increased presence of *Lactobacillus* and *Lachnospiraceae* and the decreased presence of *Desulfovibrionaceae*. Moreover, the elevated GSH levels in intestinal tissues observed following metformin treatment may originate from the gut microbiota, as indicated by the upregulation of the *GshF* gene.

Intestinal barrier dysfunction due to IIRI can lead to systemic inflammation and multiple organ damage, significantly worsening the prognosis [19, 20]. Previous studies have indicated that intestinal iron overload, such as that induced by ferric citrate, damages epithelial villi and goblet cells, leading to reduced expression of tight junction proteins [21]. In our research, we observed that the reduction in tight junction proteins and mucin due to IIRI was significantly reversed by metformin. The IIRI was associated with significant iron accumulation in ileal cells and elevated levels of TFR1 and ACSL. Moreover, GPX4, SLC7 A11, and GSH were decreased, indicating a compromised GPX4/GSH system. These findings align with previous studies showing that GPX4 undergoes a rapid decline in IIRI models, suggesting that lipid peroxides eventually impair GPX4 expression

(See figure on next page.)

Fig. 5 Metformin modulates the gut microbiota to increase GSH synthesis during IIRI. **A**–**C** The Ace, Chao, and Shannon indices were used to assess alpha diversity. **D** Microbial community composition at the phylum level. **E** Changes in microbial proportions at the genus level. **F** Predicted metabolic pathways based on the KEGG database. **G** Comparison of GSH concentrations in mouse ileum excrement across different groups. **H** GSH production by *Lactobacillus murinus* in L-NAC-MRS broth compared with that in blank MRS broth. **I** Relative mRNA expression levels of *GshF* in L-NAC-MRS broth versus blank MRS broth. **J** Fe and GSH levels in the ileal tissue of IIRI + LM mice. **K** H&E staining of tissues from IIRI and IIRI + LM group mice. (L–M) Western blot analysis of changes in ACSL4, TFR1, and GPX4 induced by *Lactobacillus murinus* gavage. The data are presented as the means ± SEMs ($n = 6$/group for A-C, G, $n = 4$/group for **J** and $n = 3$/group for **L**, **M**). *$p < 0.05$, **$p < 0.01$, ***$p < 0.001$, ****$p < 0.0001$

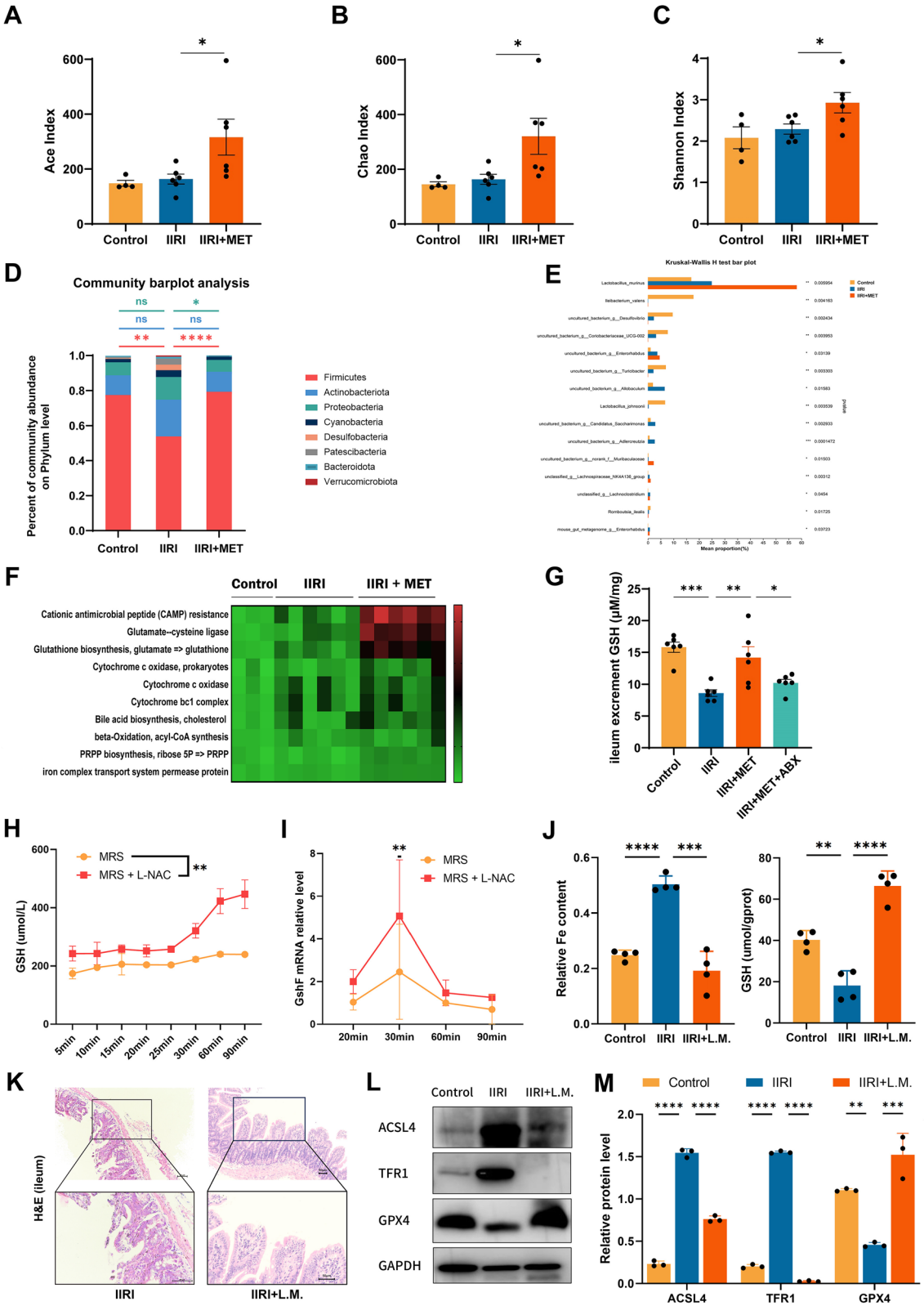

Fig. 5 (See legend on previous page.)

[8]. As GPX4 plays a critical role in detoxifying lipid peroxides, its activity is highly dependent on the availability of GSH. Depletion of GSH has been shown to induce ferroptosis, further highlighting the importance of GSH in maintaining cellular integrity during IIRI [22, 23]. Therefore, the ability of metformin to enhance GSH levels may be a key mechanism by which it attenuates intestinal ferroptosis.

In contrast to previous reports suggesting that metformin activates AMPK to inhibit IIRI-induced autophagy [24, 25], our study revealed no significant change in AMPK expression following metformin treatment. However, we observed significant increases in the abundance of *Lactobacillus*, *Lachnospiraceae*, and *Oscillospiraceae* and decreases in *Erysipelotrichaceae* and *Desulfovibrionaceae* in metformin-treated mice. The gut microbiota is crucial for maintaining host homeostasis, yet it is disrupted and can contribute to the progression of IIRI injuries [26, 27]. *Lactobacillus*, particularly *Lactobacillus murinus*, whose abundance increases significantly following metformin treatment, has been shown to mitigate intestinal barrier dysfunction and lipid peroxidation [24, 28]. A recent study indicated that indole-3-lactic acid, which originates from *Lactobacillus murinus*, decreases oxidative stress and enhances intestinal stem cell growth and specialization through the control of Nrf2 [25]. This aligns with our findings in the IIRI + LM mice model, in which *Lactobacillus murinus* treatment attenuated ferroptosis to preserve the intestinal barrier, further confirming the key role of *Lactobacillus murinus* in counteracting IIRI. Conversely, *Desulfovibrionaceae* has been associated with the accumulation of blood lipid oxidation products [29]. These findings highlight the role of metformin-modulated microbiota in protecting against ferroptosis and supporting intestinal barrier function in IIRI.

According to predictions from the KEGG database, metformin has been shown to significantly increase the activity of glutamate-cysteine ligases in microbial metabolism. Our research validated elevated levels of GSH in ileal samples from mice treated with metformin. Specifically, we identified *Lactobacillus murinus* as a bacterium that produces high levels of GSH when provided with sufficient L-NAC as a substrate. GSH synthesis occurs through three pathways: the classical pathway involving GSHA and GSGB, the bifunctional enzyme pathway involving GSHF, and an alternative pathway that relies solely on GSHB [30–33]. qRT-PCR revealed upregulated expression of *GshF* in *Lactobacillus murinus*, indicating enhanced function of bifunctional enzyme pathways. The regulatory effect of metformin on the microbiota extends beyond GSH to include microbial metabolites such as short-chain fatty acids (SCFAs), which have been shown to inhibit tumor proliferation and protect against intestinal injury [34–36]. Moreover, microbial production of hydrogen sulfide by sulfur-reducing bacteria has been linked to enhanced host GSH production, suggesting that microbial antioxidative agents can regulate the host GPX4/GSH system, thereby further contributing to the protective effects [37, 38]. However, a notable limitation of this study is that the microbiota modulation of metformin take effect over a relatively long time. Since patients with intestinal ischemia usually require rapid intervention, the delayed microbiota shift may limit the clinical applicability of metformin in acute IIRI conditions. Thus, future research should explore the potential of metformin in preventing IIRI in patients with early risk factors, and develop combinatory treatments that offer both immediate and sustained protection against IIRI.

Conclusions

Overall, our study supported that metformin attenuates IIR-induced intestinal ferroptosis through modulation of the gut microbiota. Metformin modulates the gut microbiota composition, particularly by increasing *Lactobacillus murinus*, which contributed to enhanced glutathione synthesis. Our results demonstrated that the increased bifunctional GSH synthesis pathway of the microbiota plays a critical role in this protective mechanism.

Abbreviations

ACSL4	Acyl-CoA synthetase long-chain family member 4
AMPK	AMP-activated protein kinase
cDNA	Complementary DNA
DHE	Dihydroethidium
FITC	Fluorescein isothiocyanate
GPX4	Glutathione peroxidase 4
GSH	Glutathione
H&E	Hematoxylin and eosin
IBD	Inflammatory bowel disease
IIR	Intestinal ischemia/reperfusion
IIRI	Intestinal ischemia/reperfusion injury
IL	Interleukin
IR	Ischemia/reperfusion
L-NAC	L-N-acetylcysteine
LM	*Lactobacillus murinus*
MDA	Malondialdehyde
MPO	Myeloperoxidase
MUC-2	Mucin 2
OTU	Operational taxonomic unit
PCoA	Principal coordinate analysis
qRT-PCR	Quantitative real-time PCR
ROS	Reactive oxygen species
SCFA	Short-chain fatty acid
SEM	Standard error of the mean
SLC7 A11	Solute carrier family 7 member 11
TFR1	Transferrin receptor 1
TNB	5-Thio2-nitrobenzoic acid
TRPV1	Transient receptor potential vanilloid 1
VDAC	Voltage-dependent anion channel

Supplementary Information

The online version contains supplementary material available at https://doi.org/10.1186/s12916-025-04119-6.

Additional file 1: Table S1. Primer sequences used in qRT-PCR analysis.

Additional file 2: Figure S1. Mice grouping and treatment.

Additional file 3.

Acknowledgements
Not applicable.

Authors' contributions
F.W. conceived and supervised the study. W.Y. and W.W. contributed to the methodology. X.W., J.X., Z.S., J.Z., Q.H., and E.Z. performed the investigation. X.W. and C.W. analyzed the data. F.W., X.W., and C.W. contributed to the writing of the original draft. F.W. and C.W. reviewed and edited the manuscript. All authors read and approved the final manuscript.

Funding
This study was funded by Public Welfare Technology Research Program/Social Development Project of Zhejiang Province (Grant LGF22H030011), the Key Research and Development Program of Zhejiang Province (Grant 2021C03120), and the Wenzhou Basic Scientific Research Projects (Grant Y2023415).

Data availability
The original contributions presented in the study are publicly available. These data can be found at the following link: https://www.jianguoyun.com/p/DSDv-2sQqpz4CxjGmpoFIAA.

Declarations

Ethics approval and consent to participate
The animal study was reviewed and approved by Experimental Animal Center of Wenzhou Medical University (Approval ID: wydw2022-0032).

Consent for publication
All participants involved in the study have provided their informed consent for publication of the results.

Competing interests
The authors declare no competing interests.

Author details
[1]Institute of Microbiota and Host Inflammation-Related Diseases, School of Basic Medical Science, Wenzhou Medical University, Wenzhou, China. [2]Department of Pathology, First Affiliated Hospital of Baotou Medical College of Inner, Mongolia University of Science & Technology, Baotou, China. [3]Department of Gastroenterology, The Second Affiliated Hospital and Yuying Children's Hospital of Wenzhou Medical University, Wenzhou, China. [4]Department of Colorectal and Anal Surgery, Wenzhou People's Hospital, Wenzhou, China. [5]Department of Clinical Laboratory, The First Affiliated Hospital of Henan University of Technology, Luoyang, China.

Received: 12 July 2024 Accepted: 7 May 2025
Published online: 13 May 2025

References

1. Gonzalez LM, Moeser AJ, Blikslager AT. Animal models of ischemia-reperfusion-induced intestinal injury: progress and promise for translational research. Am J Physiol Gastrointest Liver Physiol. 2015;308(2):G63–75.
2. Hou W, Yang S, Lu J, et al. Hypothermic machine perfusion alleviates ischemia-reperfusion injury of intestinal transplantation in pigs. Front Immunol. 2023;14:1117292.
3. Niu Q, Du F, Yang X, et al. Carbon monoxide-releasing molecule 2 inhibits inflammation associated with intestinal ischemia-reperfusion injury in a rat model of hemorrhagic shock. Int Immunopharmacol. 2022;113(Pt B):109441.
4. Deng F, Hu JJ, Lin ZB, et al. Gut microbe-derived milnacipran enhances tolerance to gut ischemia/reperfusion injury. Cell Rep Med. 2023;4(3):100979.
5. Cheng J, Wei Z, Liu X, et al. The role of intestinal mucosa injury induced by intra-abdominal hypertension in the development of abdominal compartment syndrome and multiple organ dysfunction syndrome. Crit Care. 2013;17(6):R283.
6. Tilsed JV, Casamassima A, Kurihara H, et al. ESTES guidelines: acute mesenteric ischaemia. Eur J Trauma Emerg Surg. 2016;42(2):253–70.
7. Yang WS, Stockwell BR. Ferroptosis: Death by Lipid Peroxidation. Trends Cell Biol. 2016;26(3):165–76.
8. Li Y, Feng D, Wang Z, et al. Ischemia-induced ACSL4 activation contributes to ferroptosis-mediated tissue injury in intestinal ischemia/reperfusion. Cell Death Differ. 2019;26(11):2284–99.
9. Wang X, Shen T, Lian J, et al. Resveratrol reduces ROS-induced ferroptosis by activating SIRT3 and compensating the GSH/GPX4 pathway. Mol Med. 2023;29(1):137.
10. Deng F, Zhao BC, Yang X, et al. The gut microbiota metabolite capsiate promotes Gpx4 expression by activating TRPV1 to inhibit intestinal ischemia reperfusion-induced ferroptosis. Gut Microbes. 2021;13(1):1–21.
11. Frankel WL, Zhang W, Singh A, et al. Mediation of the trophic effects of short-chain fatty acids on the rat jejunum and colon. Gastroenterology. 1994;106(2):375–80.
12. Wang F, Li Q, Wang C, et al. Dynamic alteration of the colonic microbiota in intestinal ischemia-reperfusion injury. PLoS ONE. 2012;7(7): e42027.
13. Wang B, Huang Q, Zhang W, et al. Lactobacillus plantarum prevents bacterial translocation in rats following ischemia and reperfusion injury. Dig Dis Sci. 2011;56(11):3187–94.
14. Wang H, Zhang W, Zuo L, et al. Bifidobacteria may be beneficial to intestinal microbiota and reduction of bacterial translocation in mice following ischaemia and reperfusion injury. Br J Nutr. 2013;109(11):1990–8.
15. Jia Y, Cui R, Wang C, et al. Metformin protects against intestinal ischemia-reperfusion injury and cell pyroptosis via TXNIP-NLRP3-GSDMD pathway. Redox Biol. 2020;32: 101534.
16. He L. Metformin and Systemic Metabolism. Trends Pharmacol Sci. 2020;41(11):868-81
17. Zhang Y, Cheng Y, Liu J, et al. Tauroursodeoxycholic acid functions as a critical effector mediating insulin sensitization of metformin in obese mice. Redox Biol. 2022;57: 102481.
18. Li J, Sun M, Liu L, et al. Nanoprobiotics for Remolding the Pro-inflammatory Microenvironment and Microbiome in the Treatment of Colitis. Nano Lett. 2023;23(18):8593–601.
19. Vollmar B, Menger MD. Intestinal ischemia/reperfusion: microcirculatory pathology and functional consequences. Langenbecks Arch Surg. 2011;396(1):13–29.
20. Kong SE, Blennerhassett LR, Heel KA, et al. Ischaemia-reperfusion injury to the intestine. Aust N Z J Surg. 1998;68(8):554–61.
21. Luo Q, Lao C, Huang C, et al. Iron Overload Resulting from the Chronic Oral Administration of Ferric Citrate Impairs Intestinal Immune and Barrier in Mice. Biol Trace Elem Res. 2021;199(3):1027–36.
22. Yang WS, SriRamaratnam R, Welsch ME, et al. Regulation of ferroptotic cancer cell death by GPX4. Cell. 2014;156(1–2):317–31.
23. Toyokuni S, Ito F, Yamashita K, et al. Iron and thiol redox signaling in cancer: An exquisite balance to escape ferroptosis. Free Radic Biol Med. 2017;108:610–26.
24. Zheng J, Ahmad AA, Yang Y, et al. Lactobacillus rhamnosus CY12 Enhances Intestinal Barrier Function by Regulating Tight Junction Protein Expression, Oxidative Stress, and Inflammation Response in Lipopolysaccharide-Induced Caco-2 Cells. Int J Mol Sci. 2022;23(19).
25. Zhang FL, Chen XW, Wang YF, et al. Microbiota-derived tryptophan metabolites indole-3-lactic acid is associated with intestinal ischemia/reperfusion injury via positive regulation of YAP and Nrf2. J Transl Med. 2023;21(1):264.
26. Wang YH, Yan ZZ, Luo SD, et al. Gut microbiota-derived succinate aggravates acute lung injury after intestinal ischaemia/reperfusion in mice. Eur Respir J. 2023;61(2).
27. Yoshiya K, Lapchak PH, Thai TH, et al. Depletion of gut commensal bacteria attenuates intestinal ischemia/reperfusion injury. Am J Physiol Gastrointest Liver Physiol. 2011;301(6):G1020–30.

28. Ni Y, Zhang Y, Zheng L, et al. Bifidobacterium and Lactobacillus improve inflammatory bowel disease in zebrafish of different ages by regulating the intestinal mucosal barrier and microbiota. Life Sci. 2023;324: 121699.
29. Van Hecke T, De Vrieze J, Boon N, et al. Combined Consumption of Beef-Based Cooked Mince and Sucrose Stimulates Oxidative Stress, Cardiac Hypertrophy, and Colonic Outgrowth of Desulfovibrionaceae in Rats. Mol Nutr Food Res. 2019;63(2): e1800962.
30. Ganguli D, Kumar C, Bachhawat AK. The alternative pathway of glutathione degradation is mediated by a novel protein complex involving three new genes in Saccharomyces cerevisiae. Genetics. 2007;175(3):1137–51.
31. Vergauwen B, Pauwels F, Van Beeumen JJ. Glutathione and catalase provide overlapping defenses for protection against respiration-generated hydrogen peroxide in Haemophilus influenzae. J Bacteriol. 2003;185(18):5555–62.
32. Franklin CC, Backos DS, Mohar I, et al. Structure, function, and post-translational regulation of the catalytic and modifier subunits of glutamate cysteine ligase. Mol Aspects Med. 2009;30(1–2):86–98.
33. Suzuki H, Kumagai H. Gamma-glutamyltranspeptidase from Escherichia coli K-12. Seikagaku. 1989;61(6):491–6.
34. Su SH, Wu YF, Lin Q, et al. Fecal microbiota transplantation and replenishment of short-chain fatty acids protect against chronic cerebral hypoperfusion-induced colonic dysfunction by regulating gut microbiota, differentiation of Th17 cells, and mitochondrial energy metabolism. J Neuroinflammation. 2022;19(1):313.
35. Broadfield LA, Saigal A, Szamosi JC, et al. Metformin-induced reductions in tumor growth involves modulation of the gut microbiome. Mol Metab. 2022;61: 101498.
36. Pryor R, Norvaisas P, Marinos G, et al. Host-Microbe-Drug-Nutrient Screen Identifies Bacterial Effectors of Metformin Therapy. Cell. 2019;178(6):1299–312 e29.
37. Kimura Y, Goto Y, Kimura H. Hydrogen sulfide increases glutathione production and suppresses oxidative stress in mitochondria. Antioxid Redox Signal. 2010;12(1):1–13.
38. Pal VK, Bandyopadhyay P, Singh A. Hydrogen sulfide in physiology and pathogenesis of bacteria and viruses. IUBMB Life. 2018;70(5):393–410.

Publisher's Note